

# Kinetics of the Direct Synthesis of Molycarbide by Reduction-Carburization of Molybdenite in the Presence of Lime

P.M. PRASAD, P. SURYA PRAKASH RAO, S.N. SINGH, A.J.K. PRASAD, and T.R. MANKHAND

Kinetic studies were conducted on the carbon monoxide reduction of molybdenite in the presence of lime. Contrary to the expectation that the  $\text{MoS}_2(\text{s}) + \text{CaO}(\text{s}) + \text{CO}(\text{g})$  reaction will result in metal formation, molycarbide was found to form and no Mo was detected in the product. This is explained on the basis of thermochemical considerations, which indicate that the  $\text{Mo}_2\text{C}$  formation is more feasible by eight orders of magnitude. The effects of quantity of lime in the charge, CO flow rate, temperature (1123 to 1298 K), and time of reduction have been studied. Kinetic analysis reveals that the results on the  $\text{MoS}_2(\text{s})$  conversion to  $\text{Mo}_2\text{C}(\text{s})$  fit into a modified parabolic rate law. Based on the thermochemical calculations and experimental findings, the probable reaction scheme has been identified. Molycarbide appears to form by a three-successive solid-gas reaction path consisting of (1) metal formation by the  $\text{MoS}_2(\text{s}) + \text{CO}(\text{g})$  reaction followed by (2) *in-situ* carburization of Mo metal by  $\text{CO}(\text{g})$ , and finally (3) the scavenging of the  $\text{COS}(\text{g})$  by lime, resulting in  $\text{CaS}(\text{s})$ . The latter two reactions drive the overall reaction forward. Further, out of these three consecutive reactions, progress of the overall  $\text{MoS}_2 + \text{CaO} + \text{CO}$  reaction seems to be governed by the *intrinsic kinetics* of the first one. Calcium molybdate, which forms as a transitory phase, plays a significant role by modifying the linear kinetics of the  $\text{MoS}_2(\text{s}) + \text{CO}(\text{g})$  to one of parabolic nature.

## I. INTRODUCTION

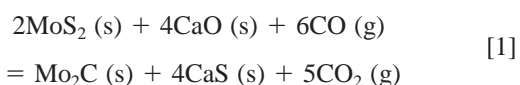
MOLYBDENUM carbide is an important material, which finds numerous applications<sup>[1-5]</sup> such as speciality cutting tools, heat-resistant hard alloys, and high-temperature solders (for specific applications), and as a catalyst in the manufacture of organic chemicals (*e.g.*, alcohols and cyclohexane). Traditionally, it is produced by three routes: (1) hydrogen reduction of its trioxide followed by carburization under hydrogen atmosphere<sup>[1,2]</sup> (2) carburization of molybdenum powder by  $\text{CO}(\text{g})$ ,<sup>[1,2]</sup> and (3) carbonaceous roasting of high-purity molybdenite in air followed by its treatment under hydrogen.<sup>[5,6]</sup> These methods suffer from several *inherent* limitations such as numerous processing steps, expensive pollution abatement measures, low recoveries, and hence the need for residue processing. A few new routes based on molten salt electrowinning from complex baths have been reported<sup>[6-9]</sup> but none has yet been commercialised. Because of the growing interest in molycarbide, its direct synthesis by a novel lime-scavenged  $\text{CO}(\text{g})$  reduction of molybdenite was attempted by Prasad and co-workers<sup>[10,11]</sup> who found that it is indeed feasible to achieve the simultaneous reduction-carburization of  $\text{MoS}_2$  resulting in the formation of 98 pct purity molycarbide. Moreover, it was noticed that the new approach is basically nonpolluting with respect to sulfur emission. Hence, compared to the

traditional or other proposed routes of producing molybdenum carbide, its direct synthesis from molybdenite looks attractive as it comprises a fewer number of processing steps. The present article deals with kinetic investigations on the  $\text{MoS}_2(\text{s}) + \text{CaO}(\text{s}) + \text{CO}(\text{g})$  reaction so as to understand the probable reaction path.

## II. THERMOCHEMICAL CALCULATIONS

### A. Thermodynamics of the Concerned Reactions

The relevant thermochemical calculations (from the data taken from References 12 and 13) concerning direct synthesis of molycarbide by the reduction of  $\text{MoS}_2(\text{s})$  by  $\text{CO}(\text{g})$  in the presence of lime ( $\text{CaO}$ ) are presented in Table I. The overall  $\text{MoS}_2(\text{s}) + \text{CaO}(\text{s}) + \text{CO}(\text{g})$  reaction resulting directly in  $\text{Mo}_2\text{C}$  formation is represented by



The preceding reaction appears to be an appropriate summation of two successive solid-gas reactions [2] and [3] (Table I). From a thermodynamic viewpoint, the reduction-carburization Reaction [2] does not appear feasible, but it may take place because of the consecutive lime sulfidation Reaction [3]. However, Reaction [2] itself consists of two successive solid/gas Reactions [4] and [5] as indicated in Table I. Fixation of sulfur as  $\text{CaS}(\text{s})$  and consequently favorable energetics (due to the highly exothermic nature of the lime-sulfidation Reaction [3]) are the other noteworthy aspects.

### B. Lime-Enhancement Diagrams

As noted in Section IIA, although the addition of lime can greatly enhance the thermodynamic feasibility of molybdenite ( $\text{MoS}_2$ ) reduction by  $\text{CO}$ , it can be effective only

P.M. PRASAD, Ex-Director, IT-BHU, and Professor of Metallurgical Engineering, Department of Metallurgical Engineering, and T.R. MANKHAND, Professor of Metallurgical Engineering, Department of Metallurgical Engineering, are with the Institute of Technology, Banaras Hindu University, Varanasi - 221 005, India. Contact e-mail: mankhand@banaras.ernet.in P. SURYA PRAKASH RAO, Assistant Professor, is with the Department of Metallurgical Engineering, Regional Engineering College, Warangal - 506 004, A.P., India. S.N. SINGH, Lecturer, is with the Department of Chemistry, H.D. Jain College, Veer Kunvar Singh University, Arrah -802 301, Bihar, India. A.J.K. PRASAD, QHF, is with the National Metallurgical Laboratory, Jamshedpur - 831 007, India.

Manuscript submitted April 9, 1998.

Table I.  $\Delta G^\circ$ ,  $\Delta H^\circ$ , and Equilibrium Constants\* for Reduction-Carburization of  $\text{MoS}_2$  at 1200 K

Reaction	Chemical Equation	$\Delta G^\circ$ (kJ mol <sup>-1</sup> )	$\Delta H^\circ$ (kJ mol <sup>-1</sup> )	$K$
(1)	$2\text{MoS}_2(\text{s}) + 4\text{CaO}(\text{s}) + 6\text{CO}(\text{g}) = \text{Mo}_2\text{C}(\text{s}) + 4\text{CaS}(\text{s}) + 5\text{CO}_2(\text{g})$	-11.55	-188.66	3.18
(2)	$2\text{MoS}_2(\text{s}) + 6\text{CO}(\text{g}) = \text{Mo}_2\text{C}(\text{s}) + 4\text{COS}(\text{g}) + \text{CO}_2(\text{g})$	+348.49	+198.54	$6.76 \times 10^{-16}$
(3)	$\text{CaO}(\text{s}) + \text{COS}(\text{g}) = \text{CaS}(\text{s}) + \text{CO}_2(\text{g})$	-90.01	-96.80	$8.23 \times 10^3$
(4)	$\text{MoS}_2(\text{s}) + 2\text{CO}(\text{g}) = \text{Mo}(\text{s}) + 2\text{COS}(\text{g})$	+179.88	+206.34	$1.48 \times 10^{-8}$
(5)	$2\text{Mo}(\text{s}) + 2\text{CO}(\text{g}) = \text{Mo}_2\text{C}(\text{s}) + \text{CO}_2(\text{g})$	-11.27	-214.14	3.09

\*Calculated using data taken from Refs. 12 and 13.

within certain limiting compositions of the reducing gas stream. This concept can be represented by what are known as *lime-enhancement diagrams*.<sup>[14,15,16]</sup> These are the plots of equilibrium  $p_{\text{CO}}$  vs CO in the reducing gas. Three such diagrams (at three different temperatures) for the system  $\text{MoS}_2\text{-CaO-CO}$  are presented in Figure 1 in which lines (a) and (b), respectively, represent the  $\text{MoS}_2(\text{s}) + \text{CO}(\text{g})$  (Reaction [4]) and  $\text{CaO}(\text{s}) + \text{COS}(\text{g})$  (Reaction [3]). At any temperature, the intersection point of the said two lines corresponds to the critical gas composition ( $p_{\text{CO}}^{\text{crit}}$ ) below which the lime-scavenged CO reduction of  $\text{MoS}_2$  will not be effective. However, this regime can get modified due to the following possibilities.

- (1) The *In-situ* oxidation of the as-formed Mo metal to  $\text{MoO}_2$  by the product gas  $\text{CO}_2$  per the reaction
 
$$\text{Mo}(\text{s}) + 2\text{CO}_2(\text{g}) = \text{MoO}_2(\text{s}) + 2\text{CO}(\text{g}) \quad [6]$$
- (2) The limitation imposed by the carbon deposition reaction
 
$$2\text{CO}(\text{g}) = \text{C}(\text{s}) + \text{CO}_2(\text{g}) \quad [7]$$
- (3) The *in-situ* CO (g) carburization of the reduced metal resulting in the formation of molybcarbide by the reaction.
 
$$2\text{Mo}(\text{s}) + 2\text{CO}(\text{g}) = \text{Mo}_2\text{C}(\text{s}) + \text{CO}_2(\text{g}) \quad [5]$$

In the plots depicted in Figure 1, vertical lines (c), (d), and (e) represent the equilibrium partial pressures of CO (g) [ $p_{\text{CO}}^{\text{oxid}}$ ,  $p_{\text{CO}}^{\text{soot}}$ , and  $p_{\text{CO}}^{\text{carb}}$ ] respectively, for the Mo oxidation, carbon deposition, and Mo carburization Reactions [6], [7], and [5]. An evaluation of the plots of Figure 1 indicates that in order to effect the reduction-cum-carburization of molybdenite in the presence of lime, the composition of reducing gas has to lie in the range represented by the vertical lines (c) and (d) or (e) and (d). An important aspect that emerges is that  $p_{\text{CO}}^{\text{carb}}$  increases with temperature *viz.* vertical line (e) shifts to the right with an increase in temperature. The permissible  $\text{CO}_2(\text{g})$  content in the reducing gas stream and the relevant  $p_{\text{CO}}$  values for the various equilibria as discussed previously are given in Table II. It can be seen that in the temperature regime 1000 to 1300 K, the  $p_{\text{CO}}$  required for *in-situ* metal carburization to  $\text{Mo}_2\text{C}$  is less than the range of  $p_{\text{CO}}$  required for the successful reduction of  $\text{MoS}_2$  to metal.

### III. EXPERIMENTAL

#### A. Materials

##### 1. Molybdenite

The technical grade molybdenite concentrate of Climax Molybdenum (supplied by M/s Minworth Metals Ltd.,

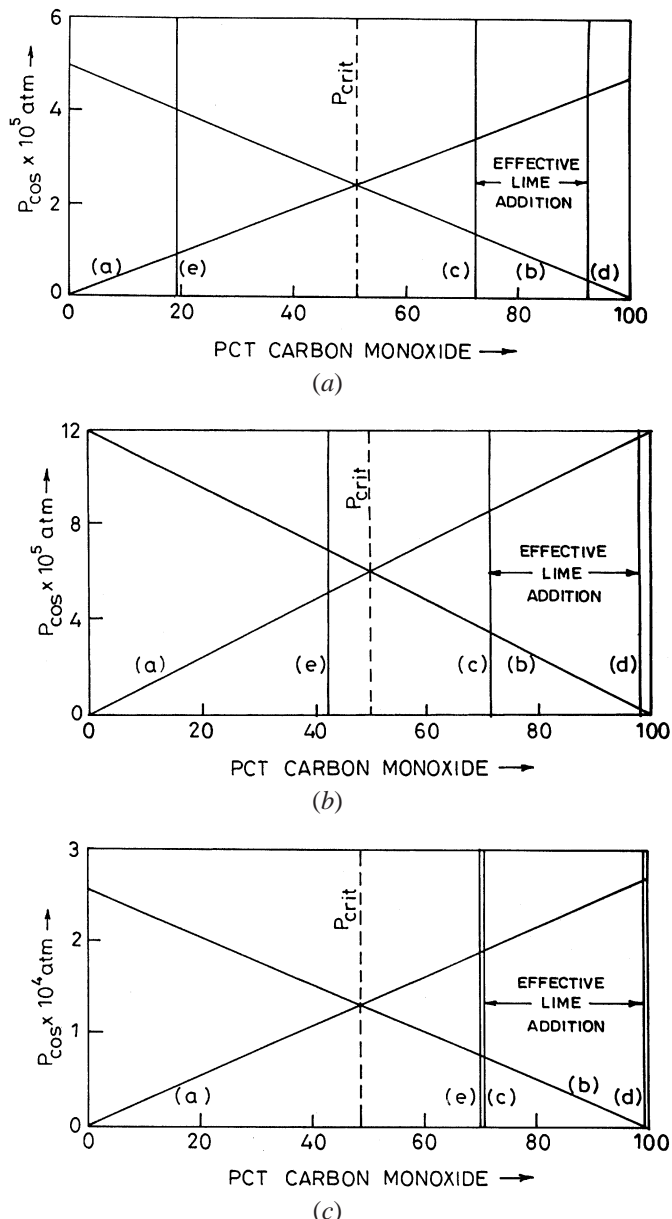


Fig. 1—*Lime-enhancement diagrams* for the system  $\text{MoS}_2(\text{s})\text{-CaO}(\text{s})\text{-CO}(\text{g})$  at (a) 1100 K, (b) 1200 K, and (c) 1300 K.

United Kingdom) has been used. X-ray diffraction (XRD) analysis revealed the presence of only  $\text{MoS}_2$  phase. Its chemical and sieve analyses are given in Table III.

**Table II. Permissible CO<sub>2</sub> at Different Temperatures for MoS<sub>2</sub> (s) + CaO (s) + CO (g) System\***

Temperature (K)	$p_{co}^{crit}$ (Pct)	$p_{co}^{oxid}$ (Pct)	$p_{co}^{soot}$ (Pct)	Permissible CO <sub>2</sub> Range (Pct)	Range of $p_{co}$ for Successful Reduction to Mo Metal (Pct)	$p_{co}^{carb}$ (Pct)	Remarks
1100	48.4	72.5	92.4	7.6 to 27.5	72.5 to 92.4	19.2	reduction-carburization can occur, resulting
1200	46.5	71.4	98.2	1.8 to 28.6	71.4 to 98.2	42.9	in the direct formation of Mo <sub>2</sub> C
1300	44.6	70.7	99.5	0.5 to 29.3	70.7 to 99.5	70.4	reduction may result in metal and/or
1400	42.7	70.1	99.8	0.2 to 29.9	70.1 to 99.8	88.6	reduction carburization to form Mo <sub>2</sub> C

\*Calculated using data taken from Refs. 12 and 13.

**Table III. Chemical and Sieve Analyses of the Molybdenite Concentrate**

A. Chemical Analysis		B. Sieve Analysis	
Constituents	Pct	Particle Size (mm)	Weight (Pct)
Mo	58.88	+0.100	1.5
S	39.44	-0.100, +0.080	3.8
Fe	0.17		
Insolubles	0.27	-0.080, +0.063	4.9
MoO <sub>3</sub>	0.01	-0.063, +0.048	10.4
C	1.00		
Oil + H <sub>2</sub> O	0.02	-0.048	79.4

**Table IV. Chemical and Sieve Analyses of Lime Powder**

A. Chemical Analysis		B. Sieve Analysis	
Constituent	Pct	Particle Size (BSS mesh)	Weight (Pct)
CaO	99.5	+22	1.3
Impurity	0.3	-22, +60 -60, +72 -72, +100 -100, +200 -200	6.5 7.9 19.8 24.4 40.1

**Table V. CO<sub>2</sub> Content in the Generated Carbon Monoxide Gas**

Gas Flow Rate (cm <sup>3</sup> s <sup>-1</sup> )	CO <sub>2</sub> in the Gas* (Pct)
1.67	12.50
3.33	13.08
8.33	14.83
13.33	16.30

\*Average value of five runs.

## 2. Calcium oxide

For each reduction test, the CaO required was prepared from the G.R. grade calcium carbonate (supplied by M/s Sarabhai M. Chemicals) by its calcination at 1273 K for 7.2 ks. Its chemical and sieve analyses are included in Table IV.

## 3. Carbon monoxide

Gas was generated by the carbon (devolatilized charcoal) + CO<sub>2</sub> (g), reaction at 1323 K, as described by Mohan *et al.*<sup>[17]</sup> The gas was analyzed for its CO<sub>2</sub> content by the Orset apparatus,<sup>[18]</sup> and it is presented in Table V.

## B. Procedure

The reduction experiments have been conducted using a Cahn-1000\* micro-recording balance to which a locally

\*Cahn-1000 is a trademark of Cahn Instruments, Carritas, CA, USA.

fabricated thermogravimetric assembly was hooked up. The silica reaction tube of the T.G. assembly was placed in a vertically movable Kanthal A<sub>1</sub> wound resistance furnace. For each reduction test, an appropriate MoS<sub>2</sub> + CaO mixture of predetermined proportion was taken in a silica crucible, which itself was suspended from the Cahn balance, such that it was in the constant temperature zone of the furnace. Before the startup of any reduction test, the system was flushed with high-purity nitrogen gas and the furnace temperature raised to the preset value (determined by prior experimentation) and then the CO (g) was admitted into the experimental set-up.

Progress of the reduction (MoS<sub>2</sub> conversion) has been followed by recording the mass change of the sample as a function of time. The off-gas from the reduction assembly was passed through two scrubbers containing standard ammoniacal cadmium chloride solution to determine sulfur emission<sup>[19]</sup> (as COS) into the off-gas. The scrubbed off-gas was then burnt off at the exit end to ensure safety.

## C. XRD Examination of the Reacted Products

The products of the MoS<sub>2</sub> (s) + CaO (s) + CO (g) and the MoS<sub>2</sub> (s) + CO (g) reactions as well as MoS<sub>2</sub> (s) + CaO (s) (blank tests) were examined by the XRD technique using a JEOL\*-8030 computer-controlled powder dif-

\*JEOL is a trademark of Japan Electron Optics Ltd., Tokyo, Japan.

fractometer. Typical XRD patterns have been included elsewhere in this article. In the reduction-carburization experiments conducted in the presence of lime, the reaction products consisted of Mo<sub>2</sub>C, and CaS as well as CaO (especially when excess lime was used). On the other hand, in the direct MoS<sub>2</sub> + CO tests carried out without lime, the reaction products were found to be Mo<sub>2</sub>C\* and unreacted

\*In a few reduction tests, MoC was detected in traces. Being a less stable phase,<sup>[20]</sup> it decomposes to Mo<sub>2</sub>C:2MoC = Mo<sub>2</sub>C + C;  $K_{1200K} = 14.2$ .

MoS<sub>2</sub>. Blank tests on MoS<sub>2</sub> + CaO reveal the formation of CaMoO<sub>4</sub>, CaS, unreacted MoS<sub>2</sub>, and CaO.

## D. Calculation of the Fraction MoS<sub>2</sub> (s) Converted

The fraction MoS<sub>2</sub> converted ( $R$ ), a dimensionless quantity, has been estimated from the relationship that is derived

assuming that it proceeds *via* Reaction [1] and from the sulfur analysis of the reactant  $\text{MoS}_2$  (s).<sup>[10]</sup>

$$R = \frac{W_e}{0.1598W_s}$$

where

$W_e$  = experimental mass loss and

$W_s$  = mass of  $\text{MoS}_2$  used in any reduction test

The sulfur emission, in the form of  $\text{COS}$  (g), is reported as sulfur (in parts per million) estimated in the off-gas.

#### IV. RESULTS

##### A. Effect of Lime

The influence of the quantity of lime on the fraction  $\text{MoS}_2$  (s) converted ( $R$ ), rate-enhancement, and accompanying sulfur emissions (as  $\text{COS}$ ) into off-gas is shown in Figure 2, Tables VI and VII, respectively. Direct reduction of the  $\text{MoS}_2$  in the absence of lime (Figure 2) is seen to be negligible. The presence of even a stoichiometric quantity of  $\text{CaO}$  ( $\text{CaO}$  to  $\text{MoS}_2$  mole ratio of 2.0) results in a conversion of 92.4 pct under a  $\text{CO}$  flow rate of  $3.33 \text{ cm}^3 \text{ s}^{-1}$  at 1223 K in 7.2 ks. The calculated rate enhancement ratios due to lime addition (Table VI) show that the addition of  $\text{CaO}$  beyond a mole ratio of 2 does not increase the reaction rate significantly. It is also clear that lime acts as a potent sulfur scavenger by reducing the "S" level in the off-gas to a very low value, *e.g.*, 14 ppm using a  $\text{CaO}:\text{MoS}_2$  mole ratio of 4 (Table VII).

##### B. Effect of $\text{CO}$ (g) Flow Rate

It is clear from Figure 3 that the conversion rate increases substantially with the  $\text{CO}$  flow rate up to a limiting value of  $8.33 \text{ cm}^3 \text{ s}^{-1}$ . A further increase in the gas flow rate (*e.g.*,  $13.33 \text{ cm}^3 \text{ s}^{-1}$ ) does not result in any appreciable increase in the  $\text{MoS}_2$  conversion rate. However, the extent of sulfur emission (as  $\text{COS}$ ) into the off-gas is seen to increase with gas flow (Figure 4) from 0.87 to 2.25 pct.

##### C. Effect of Temperature and Time

Results on the effect of temperature and time at the  $\text{CaO}$  to  $\text{MoS}_2$  mole ratio of 4.0 (twice stoichiometric) and  $\text{CO}$  flow rate of  $3.33 \text{ cm}^3 \text{ s}^{-1}$  are shown in Figure 5. Significant reduction occurs only at temperatures  $\geq 1123$  K. As is to be expected, the fraction  $\text{MoS}_2$  converted has been found to increase with temperature. A treatment time of 6.6 ks at 1273 K is considered adequate to achieve near total conversion of the  $\text{MoS}_2$  to  $\text{Mo}_2\text{C}$ .

##### D. Temperature Dependence

In their studies on the  $\text{CO}$  reduction of  $\text{PbS}$  in the presence of lime, Rao and El-Rahaiby<sup>[21]</sup> stated that the reaction  $\text{PbS}$  (s) +  $\text{CaO}$  (s) +  $\text{CO}$  (g) is very slow compared with the  $\text{CaO}$  (s) +  $\text{COS}$  (g) reaction. They have analyzed the said reaction by assuming  $\text{PbS}$  (s) +  $\text{CO}$  (g) reaction as the rate-controlling step of the process and  $\text{COS}$  as the gaseous

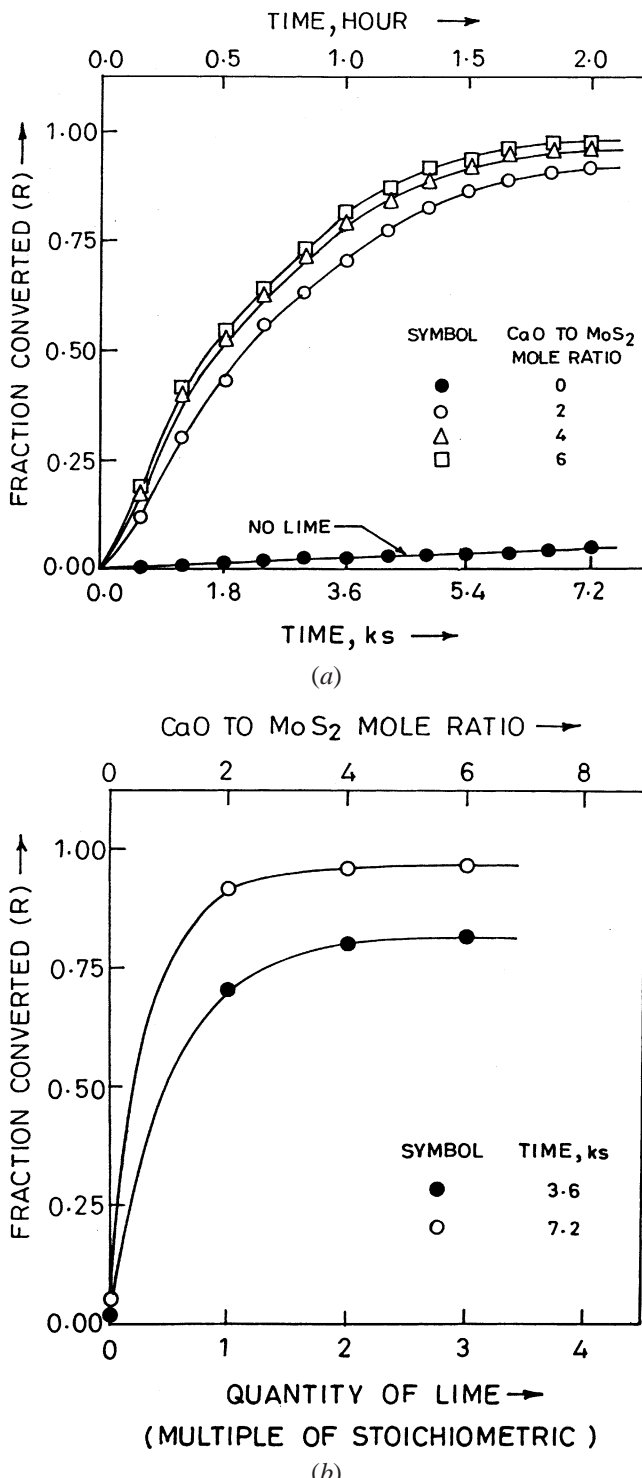


Fig. 2—(a) and (b). Effect of quantity of lime on CO reduction of molybdenite at 1223 K ( $\text{CO}$  flow rate:  $3.3 \text{ cm}^3 \text{ s}^{-1}$ ).

intermediate. Earlier, Tang<sup>[14]</sup> proposed that the  $\text{CO}$  reduction of pyrrhotite in the presence of  $\text{CaO}$  proceeds *via*  $\text{COS}$  intermediate, and the overall progress of the  $\text{FeS} + \text{CaO} + \text{CO}$  reaction is governed by the rate of the  $\text{FeS} + \text{CO}$  reaction. In the kinetic studies on several  $\text{MS}$  (s) +  $\text{CaO}$  (s) +  $\text{H}_2$  (g)/ $\text{CO}$  (g) reactions carried out in our laboratory, a similar reasoning was used; *e.g.*,  $\text{Cu}_2\text{S}$  (s) +  $\text{CaO}$  (s) +  $\text{CO}$  (g).<sup>[17]</sup>

Table VI. Estimated Ratios of Rate Increase Due to Lime Addition

Durations (ks)	Rate Enhancement at CaO to MoS <sub>2</sub> Mole Ratio of		
	2	4	6
1.8	25.5	27.6	28.0
3.6	24.5	24.9	26.0

Notes: (1) A CaO to MoS<sub>2</sub> mole ratio of 2.0 represents the theoretically required lime.

(2) Rate enhancement has been estimated by comparing the initial slopes of  $R$  vs  $t$  plots of Fig. 2.

Table VII. Effect of Lime on Sulfur Emission

Temperature: 1223 K  
CO (g) flow rate: 3.33 cm<sup>3</sup> s<sup>-1</sup>

CaO to MoS <sub>2</sub> Mole Ratio	Progress of reaction at a Treatment Time of					
	3.6 ks		7.2 ks		Sulfur in Off-Gas (Ppm)	
	Mass Loss (Pct)	R	Mass Loss (Pct)	R	Off-Gas (Ppm)	
0	1.05	0.029	1.85	0.052	112	
2	11.48	0.718	14.76	0.924	26	
4	12.79	0.800	15.40	0.964	14	
6	13.10	0.820	15.50	0.970	15	

Assuming that the reduction proceeds topochemically and the unreacted core model for spherical geometry can be applied to the present case, our reduction data has been found to fit into the Crank, Ginstling, and Brounshtein equation (modified parabolic rate law):

$$[1 - 2/3 R - (1 - R)^{2/3}] = k_p t$$

where

$R$  = fraction MoS<sub>2</sub> converted,  
 $t$  = the time of reduction, and  
 $k_p$  = the specific reaction rate constant.

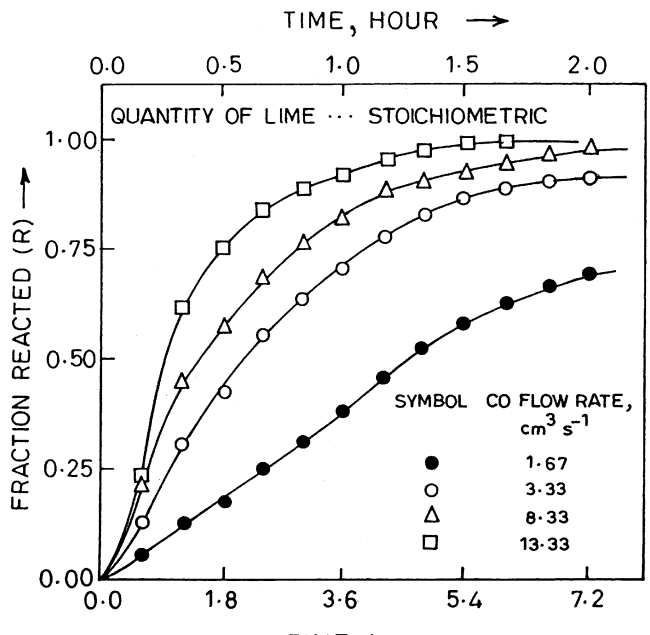
The validity of the preceding equation is evident between 20 pct reduction and 70 to 98 pct MoS<sub>2</sub> conversion depending on the temperature (Figure 6). The plot of  $\log k_p$  vs  $1/T$  (Figure 7) does indicate that the Arrhenius relationship is obeyed. By regression analysis, an activation energy value of  $193 \pm 10$  kJ mol<sup>-1</sup> has been calculated.

## V. DISCUSSION

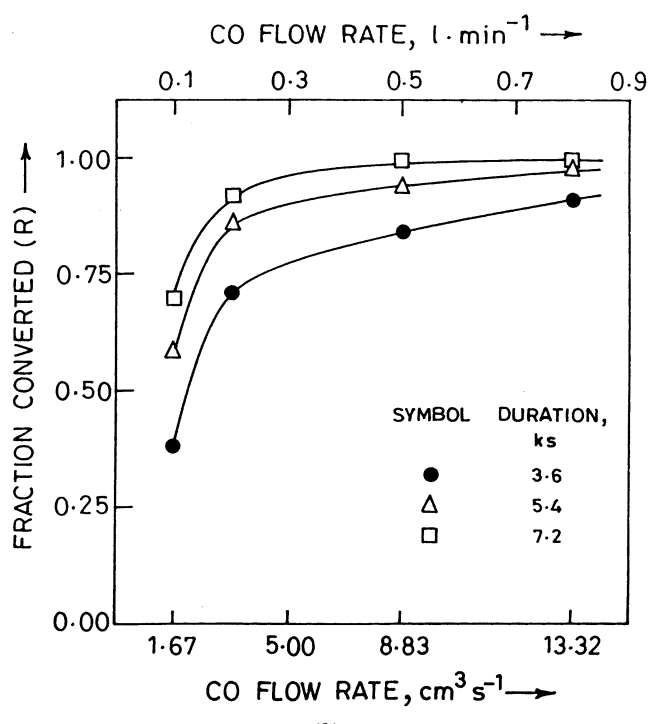
### A. Probable Reaction Path

The process under consideration, namely, the MoS<sub>2</sub> (s) + CaO (s) + CO (g) reaction resulting in the direct formation of Mo<sub>2</sub>C, may be visualized to take place *via* three reaction schemes, each of which consists of some relevant successive and/or simultaneous reactions.

- (1) *Path A* involving three consecutive (two solid/solid and one solid/gas) reactions, *viz.* MoS<sub>2</sub> + CaO resulting in MoO<sub>2</sub>, the *in-situ* sulfide-oxide interaction (MoS<sub>2</sub> + MoO<sub>2</sub>) leading to Mo metal formation, and its subsequent *in-situ* carburization by carbon monoxide.



(a)



(b)

Fig. 3—(a) and (b) Effect of CO flow rate on lime-scavenged reduction of molybdenite at 1223 K.

- (2) *Path B* consisting of a complex set of four sequential reactions involving the formation and reduction of an intermediate phase CaMoO<sub>4</sub> (See Appendix 1, which outlines this reaction scheme, and Figure 8 (d), which establishes the formation of CaMoO<sub>4</sub> in our blank tests).
- (3) *Path C* comprising three consecutive solid/gas reactions (MoS<sub>2</sub> + CO, COS + CaO, and Mo + CO).

After an in-depth scrutiny, path C is considered to be the most probable (dominant) route, which successfully explains

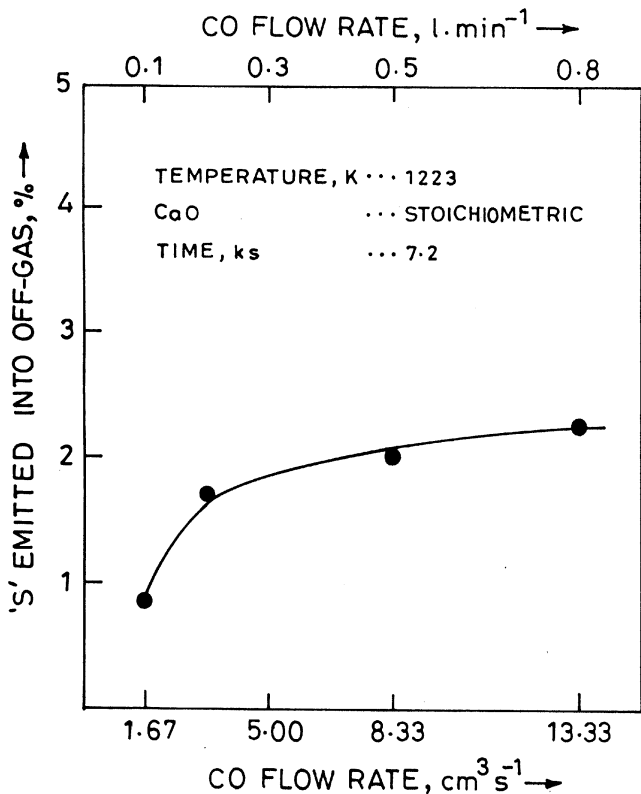
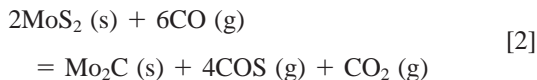


Fig. 4—Effect of CO flow rate on sulfur emission in the lime-scavenged reduction of molybdenite.

all our experimental findings; as such, this reaction scheme is now discussed.

The following is the reaction between  $\text{MoS}_2$  and CO, which leads to the formation of molycarbide,  $\text{Mo}_2\text{C}$ , and COS.



This reaction itself may consist of two consecutive solid/gas Reactions [4] and [5]



Since lime is a tested and potent scavenger for any sulfur bearing gas, it can react *in situ* with COS and fix it as CaS per Reaction [3]



Evidence for the preceding reaction scheme, consisting of the three consecutive solid/gas Reactions [4], [5], and [3], is now outlined.

- (1)  $\text{Mo}_2\text{C}$  (not the Mo metal or MoC) and CaS phases have been identified (by XRD) in the reacted products of  $\text{MoS}_2(\text{s}) + \text{CaO}(\text{s}) + \text{CO}(\text{g})$  reaction confirming the participation of lime as well as its critical role in the process (Figures 8(a) and (b)).
- (2) Tests on the reduction of molybdenite by CO in the absence of lime reveal the formation of  $\text{Mo}_2\text{C}$  (Figure 8(c))

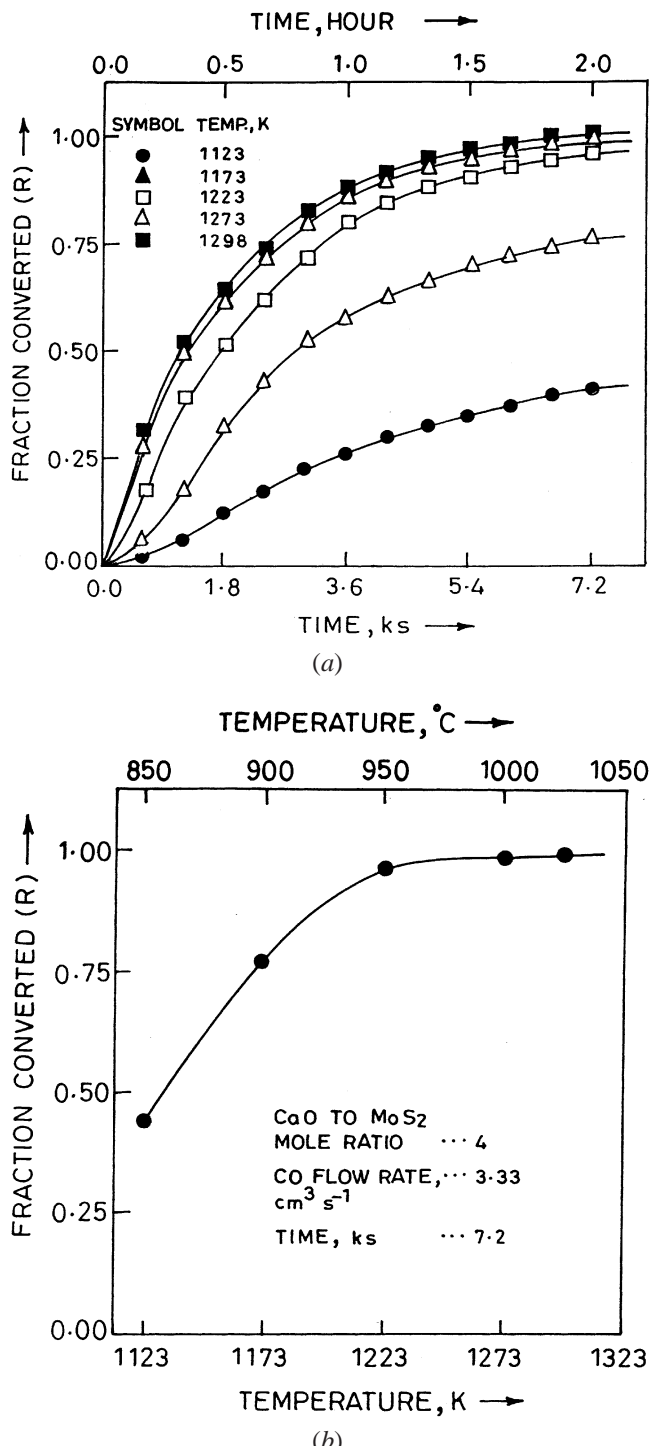


Fig. 5—(a) and (b) Effect of temperature on the lime-scavenged reduction of molybdenite by CO (lime: twice stoichiometric; and CO flow rate:  $3.33 \text{ cm}^3 \text{ s}^{-1}$ ).

- (3) Lime has been observed to play a beneficial and dominant role in enhancing the reaction rate of  $\text{MoS}_2 + \text{CO}$  by 25 times (Table VI) and also enable a drastic reduction in sulfur emission (as COS) into the off-gas (Table VII).
- (4) In all the reduction tests of the present study, the quantity of COS increased, though slightly (after a CO flow rate of  $3.33 \text{ cm}^3 \text{ s}^{-1}$ ), with the flow rate of the reducing gas (Figure 4)
- (5) Experimental mass loss data have been used to estimate

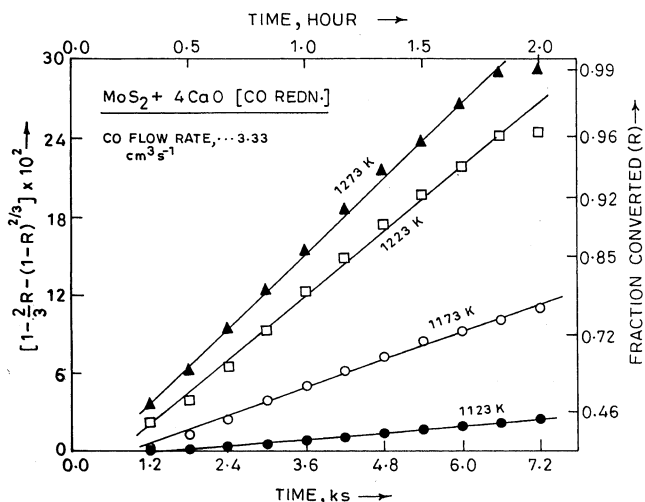


Fig. 6— $[1 - 2/3R - (1 - R)^2/3]$  vs time plots for CO reduction of molybdenite in the presence of lime.

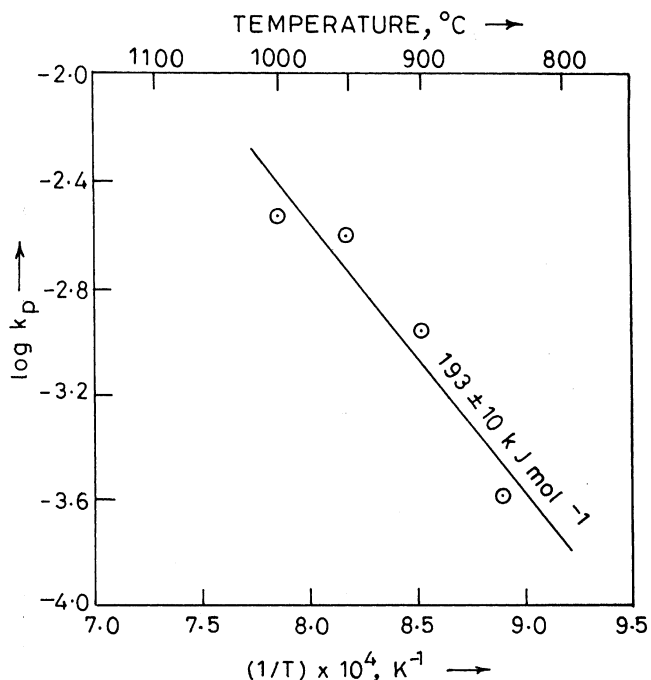


Fig. 7—Arrhenius plot for the CO reduction of molybdenite in the presence of lime.

the fraction  $\text{MoS}_2$  reacted (reduction-carburization to form  $\text{Mo}_2\text{C}$ ) values. When  $R$  was over 0.995, the product was found to be of 99 pct purity. This does confirm that the calculation of  $R$  values based on the overall Reaction [1] per the scheme considered previously is indeed justified.

#### B. Probable Mechanism

An attempt is made subsequently to analyze what may be the rate-limiting step in the path consisting of the three consecutive solid/gas Reactions [4], [5], and [3] (Table I). Yang and Chen<sup>[23]</sup> have reported that lime is a most potent sorbent for COS (CaO can effectively fix it as CaS even

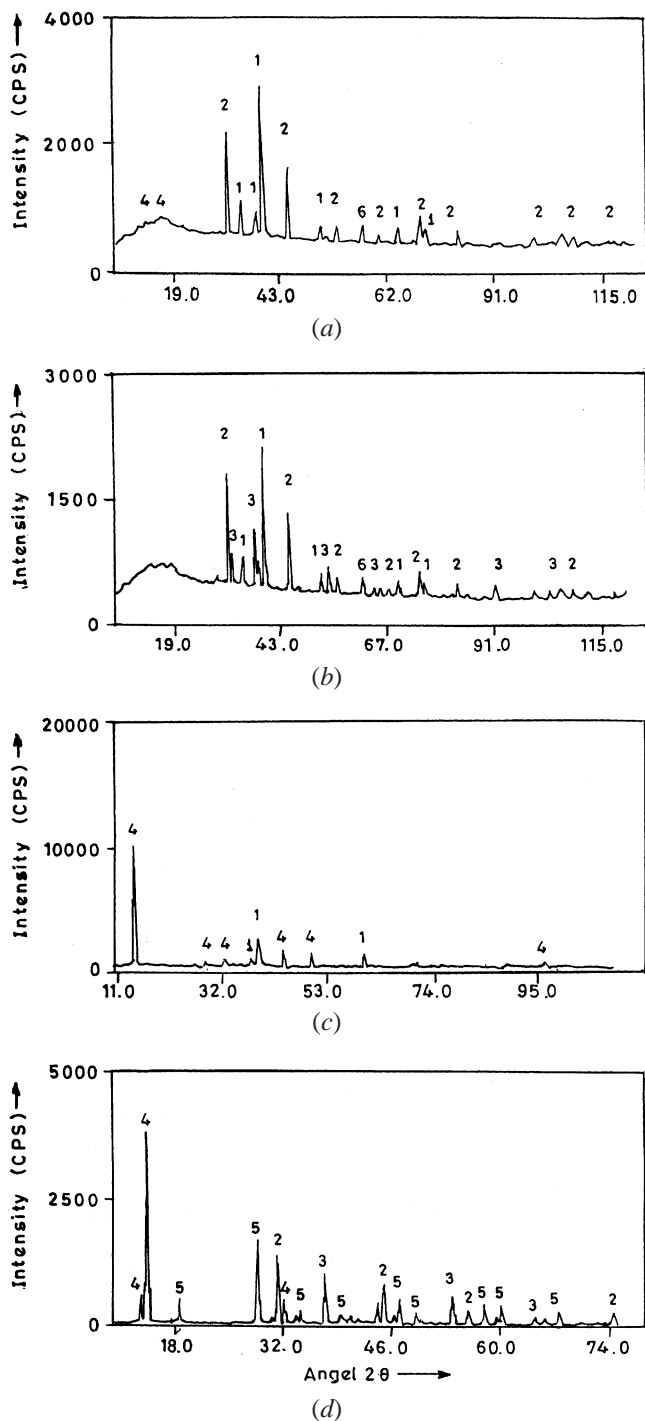


Fig. 8—Phase identification by XRD studies on reacted products at 1223 K (CO flow rate:  $8.33 \text{ cm}^3 \text{s}^{-1}$ ). (a)  $\text{MoS}_2 + \text{CaO} + \text{CO}$  (theoretical lime), (b)  $\text{MoS}_2 + \text{CaO} + \text{CO}$  (100 pct excess lime), (c)  $\text{MoS}_2 + \text{CO}$  (no lime), and (d)  $\text{MoS}_2 + \text{CaO}$  (blank test under inert gas  $\text{N}_2$ ). Legend: 1— $\text{Mo}_2\text{C}$ , 2— $\text{CaS}$ , 3— $\text{CaO}$ , 4— $\text{MoS}_2$ , 5— $\text{CaMoO}_4$ , and 6— $\text{MoC}$ .

from a dilute gas containing 0.1 pct COS + 10 pct CO + balance  $\text{N}_2$  in the temperature range 873 to 1173 (K). Rao and Prasad<sup>[10]</sup> studied the reduction-carburization of the  $\text{MoS}_2$  as well as Mo by CO. A scrutiny of relevant considerations (Table VIII), in which the ratios of (a) equilibrium constants and (b) apparent rates for the concerned reactions have been tabulated, reveal the following.

(1) From the thermodynamic viewpoint (under standard

Table VIII. Equilibrium Constants and Apparent Reaction Rates for the Proposed Reaction Path

Reaction	Chemical Equation	Equilibrium Constant at 1200 K	Fraction Reacted ( <i>R</i> )	Apparent Reaction Rate ( <i>R/t</i> )
(4)	$\text{MoS}_2(\text{s}) + 2\text{CO}(\text{g}) = \text{Mo}(\text{s}) + 2\text{COS}(\text{g})$	$1.48 \times 10^{-8}$	0.45*	$7.5 \times 10^{-4}$
(5)	$2\text{Mo}(\text{s}) + 2\text{CO}(\text{g}) = \text{Mo}_2\text{C}(\text{s}) + \text{CO}_2(\text{g})$	3.09	0.94*	$1.57 \times 10^{-2}$
(3)	$\text{CaO}(\text{s}) + \text{COS}(\text{g}) = \text{CaS}(\text{s}) + \text{CO}_2(\text{g})$	$8.28 \times 10^3$	1.00 [highly diluted COS (g)]**	$1.67 \times 10^{-2}$

\**R* values at 1173 K in 6 ks; CO flow rate:  $8.33 \text{ cm}^3 \text{ s}^{-1}$ .

\*\*Note: Data available for the  $\text{CaO}(\text{s}) + \text{COS}(\text{g})$  reaction pertain to the gas containing 0.1 pct COS only. Obviously, the rate of  $\text{CaO}(\text{s}) + \text{COS}$  ( $p_{\text{cos}} = 1$ ) will be higher.

Table IX. Ratios of Equilibrium Constants (*K*) and Apparent Reaction Rates (*k*) for the Three Selected Reactions

S. No.	Ratio of Reactions	Ratio of	
		<i>K</i> Values at 1200 K	<i>k</i> Values at 1173 K
1	<u>CaO-COS reaction (3)</u>	$5.6 \times 10^{11}$	22.2
	<u>MoS<sub>2</sub>-CO reaction (4)</u>		
2	<u>CaO-COS reaction (3)</u>	$2.7 \times 10^3$	1.1
	<u>Mo-CO reaction (5)</u>		
3	<u>Mo-CO reaction (5)</u>	$2.1 \times 10^8$	20.9
	<u>MoS<sub>2</sub>-CO reaction (4)</u>		

conditions), the lime-sulfidation (Reaction [3]) is seen to be several orders of magnitude more feasible as compared with  $\text{MoS}_2 + \text{CO}$  as well as the  $\text{Mo} + \text{CO}$  reactions.

- (2) To compare the apparent rate ratios of the three concerned reactions, we are handicapped by the lack of appropriate kinetic data for the  $\text{CaO} + \text{COS}$  (lime-sulfidation) reaction. (The data of Yang and Chen<sup>[23]</sup> pertain to experiments in which an extremely dilute (0.1 pct) COS gas was used). Nevertheless, one can look at the trends. The lime-sulfidation reaction is definitely more feasible as is evident from the ratios of the apparent reaction rates (Table IX); for example, at 1173 K, it is 22.2 times faster as compared with the  $\text{MoS}_2 + \text{CO}$  reaction.
- (3) Compared to the reduction of  $\text{MoS}_2$  by CO resulting in *in situ* Mo metal formation (Reaction 4), the consecutive reaction, *viz.* carburization of Mo by CO is seen to be much more feasible from the thermodynamic viewpoint as well as the experimentally generated kinetic data. For example, at 1200 K, the equilibrium constant value of the latter is eight orders of magnitude higher than that of the former, and our experimental work reveals that at 1173 K the former is 20.9 times faster than the latter under similar conditions.<sup>[24]</sup>

In light of the preceding analysis, it may be concluded that the progress of the lime-scavenged reaction of molybdate by carbon monoxide is governed by the *intrinsic kinetics* of the  $\text{MoS}_2 + \text{CO}$  reaction resulting initially in molybdate formation (Reaction [4]).

Now whether one considers  $\text{MoS}_2$  reduction by CO to form Mo per Reaction [4] or its direct reduction-carburization to form  $\text{Mo}_2\text{C}$  per Reaction [2], the product volume is inadequate to cover the reactant  $\text{MoS}_2$  surface (molar volume ratios of Mo/ $\text{MoS}_2$  and  $\text{Mo}_2\text{C}/2\text{MoS}_2$  are 0.282 and 0.343,

respectively; Table X). Therefore, in either case, the product layer is bound to be porous (Mo is a refractory metal). Consequently, the direct  $\text{MoS}_2 + \text{CO}$  reaction resulting in the  $\text{Mo}_2\text{C}$  product can be expected to obey linear kinetics, which is in conformity with our earlier findings<sup>[24]</sup> on the CO reduction of  $\text{MoS}_2$ .

At this juncture, it is relevant to compare the results of the reduction experiments (reduction-carburization tests on the  $\text{MoS}_2 + \text{CaO} + \text{CO}$  reaction) with those of the blank tests (*viz.*  $\text{MoS}_2 + \text{CaO}$  reaction) carried out in the absence of CO, under an inert blanket. Results of the XRD tests (Figure 8(d)) on the latter reaction clearly indicate the distinct formation of calcium molybdate (Appendix I provides an understanding of the mode of  $\text{CaMoO}_4$  formation). However, in our reduction tests, this phase is barely detected (Figures 8(a) and (b)) because, just as it forms *in situ*, it also gets reduced *in situ* (to form CaO and  $\text{Mo}_2\text{C}$ ) (Appendix I). Our studies on the CO reduction of synthetic calcium molybdate ( $\text{CaMoO}_4$ ), which were published elsewhere,<sup>[22]</sup> confirm this possibility.

As regards the influence of calcium molybdate, which seems to form as a transitory phase when  $\text{MoS}_2$  is reduced by CO in the presence of CaO, we note that the molar volume of  $\text{CaMoO}_4$  is much higher\* compared with those

\*Molar volumes ( $\text{cm}^3 \text{ mol}^{-1}$ ) of Mo,  $\text{Mo}_2\text{C}$ , and  $\text{CaMoO}_4$  have been calculated to be 9.41, 22.91, and 44.85, respectively.

of  $\text{Mo}_2\text{C}$  or Mo. Thus, even if a small amount of it is formed on the reactant sulfide ( $\text{MoS}_2$ ) particles, the molybdate can fill up the pores or voids in the product layers (Mo or  $\text{Mo}_2\text{C}$ ) resulting in an increase in the effective Pilling–Bedworth (P–B) ratio. If this happens, an impervious or at least a less porous product layer can form on the reacting  $\text{MoS}_2$  particles. Consequently, the rate law can change from one of surface control (linear kinetics) to transport/diffusional control (parabolic rate law). Indeed, it has been observed that when  $\text{MoS}_2$  is reduced by CO in the presence of lime, the reduction data fit into a parabolic rate expression (Figure 6) (as compared with the linear rate law observed for the  $\text{MoS}_2 + \text{CO}$  reaction studied in the absence of CaO).<sup>[24]</sup>

Before concluding, it is interesting to point out that the experimental work carried out in our laboratories indicates similarities with respect to (1) the rate law and nature of the products between the carbothermal reduction of  $\text{MoS}_2$  in the presence of CaO<sup>[25,26]</sup> and  $\text{CaMoO}_4$ <sup>[22]</sup> and (2) the CO reduction of  $\text{MoS}_2$  in the presence of lime (present work) and  $\text{CaMoO}_4$ .<sup>[22]</sup> But no similarity was recorded between the C and CO reduction processes of either the sulfide  $\text{MoS}_2$  (in the absence of CaO) or the molybdate,  $\text{CaMoO}_4$ . Moreover, it is also relevant to observe that the kinetic results of

Table X. Molar Volume (Pilling–Bedworth) Ratios for Reactions of Interest

Reaction	Chemical Equation	Product/Reactant	Molar Volume Ratio
(4)	$\text{MoS}_2(\text{s}) + 2\text{CO}(\text{g}) = \text{Mo}(\text{s}) + 2\text{COS}(\text{g})$	$\text{Mo}/\text{MoS}_2$	0.282
(2)	$2\text{MoS}_2(\text{s}) + 6\text{CO}(\text{g}) = \text{Mo}_2\text{C}(\text{s}) + 4\text{COS}(\text{g}) + \text{CO}_2(\text{g})$	$\text{Mo}_2\text{C}/2\text{MoS}_2$	0.343
(5)	$2\text{Mo}(\text{s}) + 2\text{CO}(\text{g}) = \text{Mo}_2\text{C}(\text{s}) + \text{CO}_2(\text{g})$	$\text{Mo}_2\text{C}/2\text{Mo}$	1.217
(3)	$\text{CaO}(\text{s}) + \text{COS}(\text{g}) = \text{CaS}(\text{s}) + \text{CO}_2(\text{g})$	$\text{CaS}/\text{CaO}$	1.708

the present investigation on the  $\text{MoS}_2(\text{s}) + \text{CaO}(\text{s}) + \text{CO}(\text{g})$  reaction bear no resemblance to the carbon reduction of  $\text{MoS}_2$  in the presence of  $\text{CaO}$  studied by us earlier<sup>[26]</sup> as well as those reported by Padilla *et al.*<sup>[27]</sup> reported recently.

## VI. CONCLUSIONS

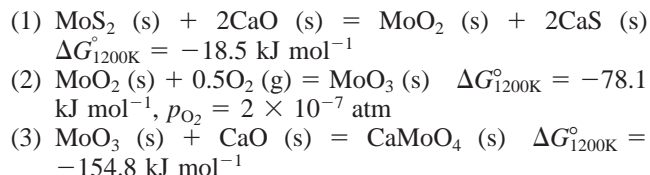
1. Contrary to the expectation that the reduction of  $\text{MoS}_2(\text{s})$  by  $\text{CO}(\text{g})$  in the presence of lime will result in the formation of moly metal, molybdenum carbide ( $\text{Mo}_2\text{C}$ ) was found to be the product of the reaction.
2. To understand the direct synthesis of  $\text{Mo}_2\text{C}(\text{s})$  by the  $\text{MoS}_2(\text{s}) + \text{CaO}(\text{s}) + \text{CO}(\text{g})$  reaction, *lime-enhancement diagrams* were constructed and the  $p_{\text{CO}}$  range required for the direct formation of  $\text{Mo}_2\text{C}$  from  $\text{MoS}_2$  has been calculated.
3. In the reduction-carburization of  $\text{MoS}_2$  by  $\text{CO}$ , the addition of lime was found to increase the rate of reaction by over 20 times and decrease the sulfur emission into the off-gas (as  $\text{COS}$ ) to negligible levels (14 ppm).
4. Results on the reduction-carburization of  $\text{MoS}_2$  were found to fit into the Crank, Ginstling, and Brounshtein equation (modified parabolic rate law), and the activation energy of the reaction was calculated to be  $193 \pm 10 \text{ kJ mol}^{-1}$  in the temperature range 1123 to 1298 K.
5. The most probable reaction path for the reduction-carburization of  $\text{MoS}_2$  in the presence of lime has been identified to be a three successive solid/gas reaction paths consisting of (1)  $\text{MoS}_2 + \text{CO}$  reaction resulting in the formation of Mo metal, (2) *in-situ* carburization of Mo by  $\text{CO}$ , and (3) fixation of the  $\text{COS}(\text{g})$  intermediate as solid  $\text{CaS}$  by its *in-situ* reaction with lime. The latter two push the reaction in the forward direction.
6. Calcium molybdate, which was detected as a transitory phase, appears to play an important role in the conversion of  $\text{MoS}_2$  to  $\text{Mo}_2\text{C}$  by causing an *in-situ* modification in the properties of the product layer. Thus, the progress of the reaction is changed from one of surface control (linear rate law) to parabolic kinetics.

## ACKNOWLEDGMENTS

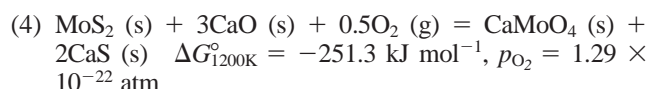
The authors acknowledge the financial support for a part of the work from the Council of Scientific and Industrial Research, Government of India, New Delhi. They are also thankful to the Head, Department of Metallurgical Engineering, Institute of Technology, Banaras Hindu University, for providing laboratory facilities.

## APPENDIX—I FORMATION OF CALCIUM MOLYBDATE ( $\text{CaMoO}_4$ ) INTERMEDIATE AND ITS REDUCTION

The reaction between  $\text{MoS}_2$  and  $\text{CaO}$  can result in the formation of  $\text{CaMoO}_4$  per the following reaction sequence:

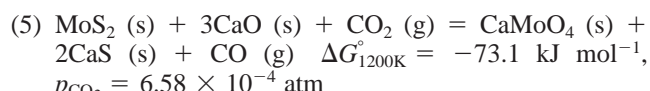


Summation of the preceding sequence yields the overall reaction



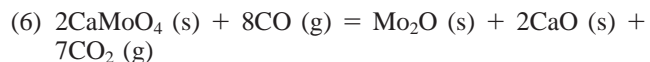
We note that for Reaction [4], the oxygen requirement is negligibly small ( $\sim 10^{-22}$  atm) and will be available *in situ* in the high-purity inert gas (nitrogen) blanket that was maintained in our experiments.

Alternatively, calcium molybdate may also form per the following reaction:



It may be noted that the  $p_{\text{CO}_2}$  required for Reaction [5] is available *in situ* in the reducing gas used in our tests (Table V).

Whatever is the mode of formation of the calcium molybdate intermediate *via* overall Reaction [4] or [5], it can get reduced per the equation given subsequently:



Our studies on the reduction of calcium molybdate by  $\text{CO}$ , which were published elsewhere,<sup>[22]</sup> do indicate that it invariably results in  $\text{Mo}_2\text{C}$  product.

## REFERENCES

1. P. Schwarkopf and R. Kieffer: *Refractory Hard Metals*, McMillion, New York, NY, 1953, p. 128.
2. T. Ya Kosolapova: *Carbides: Properties Production and Applications*, Plenum Press, New York, NY, 1971, pp. 153–59.
3. Y.B. Paderno, G.V. Somsonov, and L.M. Khernova: *Electronika*, 1959, vol. 4, p. 165.
4. G.V. Somsonov: *High Temperature Materials No. 2, Properties Index*, Plenum Press, New York, NY, 1964, p. 338.
5. A.K. Suri and C.K. Gupta: *Trans. Ind. Inst. Met.*, 1973, vol. 26 (3), pp. 19–23.
6. A.K. Suri and C.K. Gupta: *High Temp. Mater. Proc.*, 1987, vol. 7 (4), pp. 209–27.
7. J.L. Andrieux and G. Weiss: *Bull Soc. Chim., France*, 1948, vol. 15, p. 598.
8. H.J. Henein, C.L. Barber, and D.H. Beker, Jr.: *U.S. Bureau of Mines Report No. 6590*, U.S. Department of Interior, 1965.
9. A.K. Suri, T.K. Mukherjee, and C.K. Gupta: *J. Electrochim. Soc.*, 1973, vol. 120, pp. 622–24.

10. P. Surya Prakash Rao and P.M. Prasad: *Mater. Trans. JIM*, 1993, vol. 34, pp. 1229-33.
11. P.M. Prasad, T.R. Mankhand, and P. Surya Prakash Rao: *Minerals Eng.*, 1993, vol. 6 (8-10), pp. 857-71.
12. I. Barin and O. Knacke: *Thermochemical Properties of Inorganic Substances*, Springer-Verlag, New York, NY, 1973, pp. 162-64, 174, 205, 486, 488, and 491 and 492.
13. I. Barin, O. Knacke, and O. Kubaschewski: *Supplement to Thermochemical Properties of Inorganic Substances*, Springer-Verlag, New York, NY, 1977, p. 104.
14. Y.K. Tang: Ph.D. Thesis, The Ohio State University, Columbus, OH, 1976.
15. P.M. Prasad and T.R. Mankhand: in *Advances in Sulphide Smelting*, vol. 1, *Basic Principles*, H.Y. Sohn, D.B. George, and A.D. Zunkel, eds., TMS-AIME, Warrendale, PA, 1983, pp. 371-92.
16. A.R. Udupa, K.A. Smith, and J.J. Moore: *Metall. Trans. B*, 1986, vol. 17B, pp. 185-96.
17. M.K. Mohan, T.R. Mankhand, and P.M. Prasad: *Metall. Trans. B*, 1987, vol. 18B, pp. 719-25.
18. B.C. Agrawal and S.P. Jain: *A Text Book of Metallurgical Analysis*, Khanna Publishers, Delhi, 1971, p. 314.
19. R.S. Young: *Chemical Analysis in Extractive Metallurgy*, Charles Griffin Co. Ltd., London, 1971, p. 318.
20. Bruce M. Warnes and G. Simkovich: *J. Less-Common Met.*, 1985, vol. 106, p. 241.
21. Y.K. Rao and S.K. El-Rahaiby: *Chem. Eng. Sci.*, 1984, vol. 39, pp. 1157-66.
22. T.R. Mankhand, P. Surya Prakash Rao, S.N. Singh, and P.M. Prasad: *Met. Mater. Processes*, 1995, vol. 7 (2), pp. 113-20.
23. R.T. Yang and J.M. Chen: *Environ. Sci. Technol.*, 1979, vol. 13, pp. 549-53.
24. P. Surya Prakash Rao, T.R. Mankhand, and P.M. Prasad: *Mater. Trans., JIM*, 1996, vol. 37 (3), pp. 239-44.
25. P. Surya Prakash Rao: Ph.D. Thesis, Banaras Hindu University, Varanasi, 1994.
26. P. Surya Prakash Rao, T.R. Mankhand, and P.M. Prasad: *Met. Mater. Processes*, 1993, vol. 4 (4), pp. 315-22.
27. R. Padilla, M.C. Ruiz, and H.Y. Sohn: *Metall. Trans B*, 1997, vol. 28B, pp. 265-74.